Earth and Planetary Science Letters 308 (2011) 131–140

Contents lists available at ScienceDirect

Earth and Planetary Science Letters

journal homepage: www.elsevier.com/locate/epsl

High-temperature inter-mineral magnesium isotope fractionation in mantle xenoliths from the North China craton

Sheng-Ao Liu [a,b,*], Fang-Zhen Teng [b,*], Wei Yang [b,c], Fu-Yuan Wu [c]

[a] CAS Key Laboratory of Crust–Mantle Materials and Environments, School of Earth and Space Sciences, University of Science and Technology of China, Hefei, Anhui 230026, China
[b] Isotope Laboratory, Department of Geosciences and Arkansas Center for Space and Planetary Sciences, University of Arkansas, Fayetteville, AR 72701, USA
[c] State Key Laboratory of Lithospheric Evolution, Institute of Geology and Geophysics, Chinese Academy of Sciences, Beijing 10029, China

ARTICLE INFO

Article history:
Received 5 February 2011
Received in revised form 20 May 2011
Accepted 24 May 2011
Available online 12 June 2011

Editor: R.W. Carlson

Keywords:
magnesium isotopes
inter-mineral isotope fractionation
spinel
olivine
pyroxene
peridotite xenolith

ABSTRACT

To investigate the magnitude and mechanism of inter-mineral Mg isotope fractionation at mantle temperatures, we measured Mg isotopic compositions of coexisting olivine (Ol), orthopyroxene (Opx), clinopyroxene (Cpx), phlogopite (Phl) and spinel (Spl) from harzburgite, lherzolite and clinopyroxenite xenoliths in the North China craton. These xenoliths are well-characterized and formed over a wide temperature range from ~800 to 1150 °C. The coexisting Opx and Ol have constant and indistinguishable Mg isotopic compositions, with δ^{26}Mg ranging from −0.29 to −0.22‰ in Ol and from −0.28 to −0.22‰ in Opx ($\Delta^{26}Mg_{Opx-Ol} = \delta^{26}Mg_{Opx} - \delta^{26}Mg_{Ol} = -0.04$ to +0.04‰; n = 11). By contrast, Mg isotopic compositions of Cpx and Phl are variable and slightly heavier than coexisting Ol ($\Delta^{26}Mg_{Cpx-Ol} = 0$ to +0.13‰, n = 13; $\Delta^{26}Mg_{Phl-Ol} = +0.11$ to +0.20‰, n = 3). Isotope fractionations between coexisting Cpx and Ol are correlated with temperatures, implying equilibrium isotope fractionation. The degree and direction of isotope fractionations among these mantle silicates agree with theoretical predictions, suggesting that inter-mineral Mg isotope fractionation is primarily controlled by the Mg–O bond strength, with stronger bonds favoring heavier Mg isotopes. Cpx and Phl have shorter and thus stronger Mg–O bonds, and hence are isotopically heavier than coexisting Ol. Compared with coexisting silicates, δ^{26}Mg values of spinels are more variable and much heavier, ranging from +0.03 to +0.28‰. The $\Delta^{26}Mg_{Spl-Ol}$ values vary significantly from +0.25 to +0.55‰ (n = 10) and show an excellent, positive, linear correlation with $10^6/T^2$(K) [$\Delta^{26}Mg_{Spl-Ol} = 0.63 (\pm 0.12) \times 10^6/T^2(K) - 0.03(\pm 0.08)$], indicating equilibrium Spl–Ol isotope fractionation. The absence of intra-mineral isotopic variation and quantitative diffusion calculations further confirm isotope exchange equilibrium between coexisting Spl and Ol. Our results demonstrate the existence of measurable Mg isotope fractionation between mantle minerals and suggest that the large high-temperature equilibrium Spl–Ol Mg isotope fractionation in peridotite xenoliths can potentially be used as a geothermometer in mantle geochemistry.

© 2011 Elsevier B.V. All rights reserved.

1. Introduction

Whether there is detectable high-temperature inter-mineral Mg isotope fractionation between coexisting mantle minerals and whether the isotope fractionation reflects equilibrium partitioning or open-system behavior, are highly debated. Several studies reveal limited (i.e., ≤0.2‰) Mg isotope fractionation between coexisting pyroxene and olivine in fifteen mantle peridotite xenoliths (Handler et al., 2009; Wiechert and Halliday, 2007; Yang et al., 2009). By contrast, two studies, each based on two samples, reported significant (up to ~0.4‰) Mg isotope fractionation between coexisting pyroxene and olivine (Chakrabarti and Jacobsen, 2010; Young et al., 2009). Specifically, Young et al. (2009) reported up to 0.8‰ Mg isotope fractionation between coexisting spinels and olivines in two peridotite xenoliths and interpreted the large isotope fractionation as a result of equilibrium isotope partitioning.

The direct way to solve the above debates is to experimentally calibrate Mg isotope fractionation factors in mantle minerals and melts. However, to date, such studies are still not available. Alternatively, equilibrium isotope fractionation is temperature-dependent, with the magnitude of isotope fractionation decreasing with increasing temperature. Therefore, inter-mineral Mg isotope fractionations between coexisting minerals in a suite of natural samples that formed over a large range of temperature, if any, should show temperature-dependent variation. None of those earlier studies mentioned above, however, have taken into account the temperature effects.

Here, we measured coexisting olivine, orthopyroxene, clinopyroxene, phlogopite, and spinel from thirteen mantle xenoliths in the North

* Corresponding authors.
E-mail addresses: lsa@mail.ustc.edu.cn (S.-A. Liu), fteng@uark.edu (F.-Z. Teng).

0012-821X/$ – see front matter © 2011 Elsevier B.V. All rights reserved.
doi:10.1016/j.epsl.2011.05.047

China craton that formed over a wide (>300 °C) temperature range. Our results demonstrate that there are detectable equilibrium Mg isotope fractionations between coexisting spinel/clinopyroxene/phlogopite and olivine, and undetectable fractionation between coexisting orthopyroxene and olivine in mantle xenoliths; the large spinel–olivine Mg isotope fractionation can potentially be used as a geothermometer in mantle geochemistry; and the Earth, as represented by these mantle xenoliths, has a chondritic Mg isotopic composition.

2. Samples

Samples studied here include olivine (Ol), orthopyroxene (Opx), clinopyroxene (Cpx), spinel (Spl) and phlogopite (Phl) from thirteen peridotite and clinopyroxenite xenoliths hosted by three Cenozoic volcanoes in the North China craton (NCC). All samples represent residues after the extraction of partial melts in the spinel stability field, and are well-characterized, with petrology, mineralogy, chemical and isotopic compositions presented in previous studies (Wu et al., 2006; Zhao et al., 2007).

2.1. Kuandian peridotite xenoliths

The Kuandian peridotite xenoliths were collected from the Huangyishan alkaline basalts in the NCC (Wu et al., 2006). They range from refractory harzburgite to relatively fertile lherzolite, and show a complex distribution in the rare earth element (REE) patterns, with depletion to remarkable enrichment of light REEs relative to heavy REEs, suggesting various degrees of metasomatism. Based upon the two-pyroxene Ca thermometry of Brey and Köhler (1990), the Kuandian peridotites formed over a large range of equilibrium temperature from 807 to 1150 °C, with the amphibole-bearing lherzolite (HY2-06) having the lowest temperature of 807 °C (Wu et al., 2006). Uncertainties of the estimated equilibrium temperatures are ±15 °C (1σ) that are independent of compositional parameters (Brey and Köhler, 1990).

The mineral modes of Kuandian peridotites are: 52–75% Ol, 23–31% Opx, 3–16% Cpx, and 1–3% Spl, with sample HY2-06 containing ~2% amphibole (Wu et al., 2006). The olivine separates have Fo contents [=molar $100\times Mg/(Mg+Fe^{2+})$] ranging from 90.2 to 91.8, and represent residues after the extraction of various extents of partial melts in the spinel stability field (Wu et al., 2006). Clinopyroxene separates have trace element patterns similar to bulk peridotites, indicative of various degrees of enrichment due to secondary metasomatism. The spinels exhibit relatively uniform contents of MgO (19.4 to 22.3 wt.%) and FeO (10.4 to 12.1 wt.%), but large variations in Al_2O_3 (43.3 to 56.8 wt.%), Cr_2O_3 (8.7 to 25.7 wt.%), and Cr# [=molar $100\times Cr/(Cr+Al)$, from 9.0 to 28.5] (Wu et al., 2006).

Olivine, Opx, Cpx and Spl from ten Kuandian peridotite xenoliths were chosen for Mg isotopic analysis. Magnesium isotopic compositions of these bulk peridotites were reported in Teng et al. (2010a).

2.2. Hannuoba olivine–clinopyroxenite xenolith

The Hannuoba phlogopite-bearing olivine–clinopyroxenite (DMP06-50) was collected from the Cenozoic Hannuoba volcano in the NCC. This sample is composed of 20% Ol, 2% Opx, 60% Cpx, 5% Spl, and 13% phlogopite, with a two-pyroxene Ca equilibrium temperature of 965 °C (Zhao et al., 2007). As shown by the high modes of phlogopite and clinopyroxene as well as chemical compositions of clinopyroxene, this clinopyroxenite sample was subject to strong metasomatism. The clinopyroxene separates display a strong LREE-enriched pattern with $(La/Yb)_N=12$ (Zhao et al., 2007) and the phlogopite is enriched in alkaline elements, Ti, Cr, and radiogenic Sr isotopes, suggesting strongly secondary metasomatism by H_2O-rich fluids and formation through interactions of melts with lherzolites (Zhao et al., 2007).

Here, Ol, Opx, Cpx, and Phl from this olivine–clinopyroxenite sample were separated for Mg isotopic analysis.

2.3. Sanyitang peridotite xenoliths

The Sanyitang peridotite xenoliths were collected from Cenozoic basalts from the Sanyitang volcano in Jining area of the NCC. Two peridotite samples (SYT06-41 and SYT06-42) were chosen for Mg isotopic analysis in this study. Both are phlogopite-bearing spinel lherzolites and have similar two-pyroxene Ca equilibrium temperatures (941 and 945 °C) (Zhao et al., 2007). The mineral mode is 60% Ol, 15% Opx, 13% Cpx, and 10% phlogopite in sample SYT06-41, and 58% Ol, 17% Opx, 10% Cpx, and 13% phlogopite in sample SYT06-42. Significant metasomatism also occurred for these two samples, as indicated by their high phlogopite modes.

Magnesium isotopic compositions of Ol, Opx and Cpx from these two peridotites were analyzed by Yang et al. (2009). Here we analyzed the phlogopite separates and re-analyzed Ol and Cpx from these two spinel lherzolite samples.

3. Analytical methods

Dissolution of silicate minerals, column chemistry and instrumental analysis followed procedures reported in previous studies (Li et al., 2010, 2011; Liu et al., 2010; Teng et al., 2007, 2010a,b; Yang et al., 2009). Only a brief description is given below.

Approximately 1–3 mg Ol, Opx, Cpx and Phl were dissolved in a mixture of Optima-grade HF + HNO_3 + HCl at 160 °C. Spinel separates were crushed to 40–60 mesh size and handpicked under a binocular microscope. Six to eight unaltered grains (weighted 1–2 mg) of each spinel sample were then pulverized in an agate mortar with an agate pestle, and cleaned with Milli-Q water (18.2 MΩ cm) three times. For some peridotite samples, different batches of spinel separates from the same sample were analyzed to evaluate possible intra-mineral Mg isotopic variation. The crushed spinel powder was completely dissolved in 1:1 HCl + HF in high-pressure bombs in a muffle furnace at 220 °C for about 30 h. In preparation for column chemistry, all sample solutions were dried down, refluxed with concentrated Optima HNO_3 at 160 °C, and finally dissolved in 1 N HNO_3.

Magnesium was purified by cation exchange chromatography using Bio-Rad AG50W-X8 (200–400 mesh) resin. Each sample was processed through column chemistry twice in order to obtain a pure Mg solution with concentration ratios of other cations to Mg less than 0.05. Some spinel samples were processed through column chemistry four times to further evaluate the efficiency of our procedure on separation of matrix elements (e.g., Cr) from Mg. The final solutions were heated to dryness in a vented laminar-flow hood and dissolved in 3% HNO_3 for mass spectrometry.

Magnesium isotopic ratios were measured by the sample-standard bracketing method using a *Nu Plasma* multi-collector inductively coupled plasma mass spectrometer (MC-ICP-MS) at the Isotope Laboratory of the University of Arkansas. At least one well-characterized standard was run during each batch of sample analysis. Magnesium isotope data are reported in the δ-notation relative to Mg isotope standard DSM3: $\delta^x Mg=[(^xMg/^{24}Mg)_{sample}/(^xMg/^{24}Mg_{DSM3})-1]\times 10^3$, where x refers to 25 or 26.

The long-term external reproducibility on $^{26}Mg/^{24}Mg$ ratio measurement is better than ±0.07‰ (2 SD), based on replicate analyses of natural and synthetic standard solutions (Teng et al., 2010a). An in-house olivine standard from Kilbourne Hole (KH) and seawater were analyzed multiple times for accuracy check during the course of this study. Multiple analyses of KH yielded an average $\delta^{26}Mg$ value of −0.27 ± 0.04 (n = 13; 2 SD, Table 1), identical to that ($\delta^{26}Mg$ = −0.27 ± 0.07; 2 SD) reported by Teng et al. (2010a) and Liu et al. (2010). Seawater analyzed in this study yielded $\delta^{26}Mg$ of −0.86 ± 0.05 (2 SD), in agreement with previously reported values of −0.85 ± 0.05 (2 SD) (Li

Table 1
Magnesium isotopic compositions of reference materials analyzed in this study.

Reference material	δ^{26}Mg	2 SD	δ^{25}Mg	2 SD	n
KH-olivine	−0.26	0.07	−0.14	0.04	4
Replicate	−0.24	0.05	−0.11	0.03	2
Replicate	−0.25	0.05	−0.13	0.05	2
Replicate	−0.30	0.07	−0.16	0.05	2
Replicate	−0.27	0.06	−0.11	0.04	2
Replicate	−0.26	0.06	−0.12	0.05	4
Replicate	−0.27	0.05	−0.11	0.05	2
Replicate	−0.28	0.07	−0.12	0.05	4
Replicate	−0.32	0.05	−0.14	0.04	2
Replicate	−0.30	0.07	−0.15	0.07	2
Replicate	−0.28	0.08	−0.14	0.04	2
Replicate	−0.28	0.08	−0.14	0.04	2
Replicate	−0.26	0.04	−0.16	0.05	2
Average (n = 13)	−0.27	0.04	−0.13	0.04	
Seawater	−0.86	0.04	−0.45	0.05	2

KH-olivine is an in-house standard that has been analyzed through whole-procedural column chemistry and instrumental analysis, and has $\delta^{26}Mg = -0.27 \pm 0.07$ and $\delta^{25}Mg = -0.14 \pm 0.04$ (2 SD) relative to DSM3 (Li et al., 2010; Liu et al., 2010; Teng et al., 2010a). 2 SD indicates 2 times the standard deviation of the population of n (times) repeat measurements of a sample solution. Replicate denotes repeating sample dissolution, column chemistry and instrumental analysis.

et al., 2010), −0.84 ± 0.05 (2 SD) (Teng et al., 2010b), −0.83 ± 0.06 (2 SD) (Teng et al., 2010a), and −0.82 ± 0.06 (2 SD) (Foster et al., 2010). Finally, Ol and Cpx separates from two peridotite xenoliths in Sanyitang that were previously analyzed by Yang et al. (2009) in the same laboratory were re-analyzed here. The results analyzed here agree well with those reported in Yang et al. (2009) within ±0.04‰ on δ^{26}Mg (Table 2), further confirming our long-term (>20 months) analytical reproducibility.

4. Results

Magnesium isotopic compositions are reported in Table 1 for reference materials (KH olivine and seawater), and Table 2 for mineral separates (Ol, Opx, Cpx, Spl and Phl) and bulk peridotites, along with mineral modes, MgO contents and estimated equilibrium temperatures. Magnesium isotopic compositions for all mineral separates are plotted as a function of estimated equilibrium temperatures in Fig. 1. The inter-mineral Mg isotopic difference between two coexisting minerals is defined as $\Delta^{26}Mg_{X-Y} = \delta^{26}Mg_X - \delta^{26}Mg_Y$, where X and Y refer to different minerals. Mineral Y refers to Ol exclusively in this study. All samples including reference materials analyzed in this study fall on a single isotopic mass-dependent fractionation line with a slope of 0.512 (not shown).

4.1. Ol, Opx and Cpx in Kuandian and Sanyitang peridotites and Hannuoba clinopyroxenite

Olivine samples from Kuandian and Sanyitang peridotites and Hannuoba olivine–clinopyroxenite have homogeneous Mg isotopic compositions, with δ^{26}Mg varying from −0.29 to −0.22 (n = 13) (Fig. 1). Orthopyroxene separates also have homogenous Mg isotopic compositions, with δ^{26}Mg varying from −0.28 to −0.22 (n = 11) (Fig. 1). Clinopyroxene separates show slightly heterogeneous Mg isotopic compositions, with δ^{26}Mg ranging from −0.25 to −0.14 (n = 13) (Fig. 1). The $\Delta^{26}Mg_{Cpx-Ol}$ values vary from 0.0 to +0.13‰ (n = 13) and the $\Delta^{26}Mg_{Opx-Ol}$ values vary from −0.04 to +0.04‰ (n = 11) (Fig. 2a, b).

4.2. Phlogopite in Sanyitang peridotites and Hannuoba clinopyroxenite

δ^{26}Mg of phlogopite from Hannuoba clinopyroxenite (−0.11) is slightly higher than that of coexisting olivine (−0.22), with $\Delta^{26}Mg_{Phl-Ol} = +0.11$‰ (Fig. 3). δ^{26}Mg values of two phlogopites from Sanyitang peridotites are −0.15 and −0.06, yielding $\Delta^{26}Mg_{Phl-Ol}$ of +0.12 and +0.20‰, respectively (Fig. 3).

4.3. Spinel in Kuandian peridotites

All spinels from Kuandian peridotites have positive δ^{26}Mg values varying significantly from +0.03 to +0.28 (n = 10) (Fig. 1). The $\Delta^{26}Mg_{Spl-Ol}$ values show a large variation from +0.25 to +0.55‰ (n = 10) (Fig. 4). Different batches of spinels, with each containing 6–8 single grains from the same peridotite sample, have identical Mg isotopic compositions within analytical uncertainty (Fig. 1).

5. Discussion

In this section, we first evaluate whether these inter-mineral Mg isotope fractionations in mantle xenoliths are in equilibrium or not. We then discuss the implications of these inter-mineral Mg isotope fractionations on geothermometry and Mg isotopic composition of the Earth.

5.1. Theoretical considerations of equilibrium magnesium isotope fractionation in mantle rocks

Theoretical studies suggest that equilibrium inter-mineral isotope fractionation is primarily controlled by the bonding environment of the element of interest, with stronger bonding favoring incorporation of heavy isotopes (Bigeleisen and Mayer, 1947; Urey, 1947). In general, stronger bonding is associated with lower coordination number (CN). This theoretical prediction has been qualitatively used to explain inter-mineral stable isotope fractionation in igneous and metamorphic rocks for e.g., Li isotopes (Teng et al., 2006), Mg isotopes (Li et al., 2011; Liu et al., 2010; Young et al., 2009), Fe isotopes (Shahar et al., 2008) and Ca isotopes (Huang et al., 2010).

As discussed in Liu et al. (2010), the coordination of Mg bonded to O in silicate minerals e.g., olivine, orthopyroxene, clinopyroxene, hornblende, and biotite, is the same, i.e., CN = 6, whereas the coordination of O bonded to Mg is slightly different. This suggests similar Mg–O bond strength among these minerals and hence rules out the possibility of any large equilibrium inter-mineral Mg isotope fractionation at high temperatures. Nonetheless, small inter-mineral fractionation can still occur due to the slightly different bond strength produced by the different CN of oxygen. In contrast to above silicates, the CN of Mg in spinel ($MgAl_2O_4$) is 4 (i.e., a much shorter Mg–O bond than that in mantle silicates), whereas the CN of Mg in garnet is 8 (i.e., a much longer Mg–O bond than that in other mantle minerals). The distinct coordination of Mg and Mg–O bonding imply that spinel should have much heavier whereas garnet should have much lighter Mg isotopic compositions than coexisting silicate minerals (Ol, Opx, Cpx, and Phl) when equilibrium Mg isotope exchange is achieved. Hence, based on the coordination of Mg and O in mantle minerals, Mg isotopic composition in coexisting mantle minerals can be predicted as the following sequence of enriched ^{26}Mg: Spl ≫ Phl > Opx and Cpx > Ol ≫ garnet. This sequence, though qualitatively, agrees well with the quantitative calculation done by Schauble (2011), which predicted a sequence of enriched ^{26}Mg in the following order: Spl ≫ Cpx > Opx > Ol. The slight enrichment of Cpx in δ^{26}Mg than Opx has been discussed in detail in Schauble (2011). It is worth to mention that although quantitative calculation is not available on Mg isotope fractionation involving garnets, recent studies of orogenic eclogites have found large equilibrium inter-mineral Mg isotope fractionation with garnets ~1.1‰ lighter than coexisting omphacites (Li et al., 2011).

Table 2
Magnesium isotopic compositions of silicate minerals and spinels from peridotite and clinopyroxenite xenoliths in the North China craton.

Sample	Rock type	T (°C)[a]	Mineral[b]	Modal	MgO	δ^{26}Mg	2 SD	δ^{25}Mg	2 SD	N[c]
Kuandian										
HY2-01	Lherzolite	966	Opx	0.33	33.91	−0.25	0.05	−0.13	0.05	4
			Cpx	0.08	16.43	−0.25	0.06	−0.11	0.06	10
			Olivine	0.58	50.09	−0.26	0.04	−0.16	0.01	2
			Spinel	0.02	20.08	+0.09	0.06	+0.04	0.05	4
			Duplicate[d]			+0.08	0.04	+0.06	0.05	2
			Average			+0.09	0.03	+0.05	0.02	
			Whole-rock[e]	1.00	41.70	−0.25	0.04	−0.15	0.05	
			Whole-rock[f]			−0.23	0.06	−0.14	0.05	4
HY1-01	Harzburgite	991	Opx	0.27	34.01	−0.25	0.05	−0.13	0.05	4
			Cpx	0.04	16.41	−0.22	0.03	−0.12	0.05	10
			Olivine	0.69	50.66	−0.23	0.03	−0.15	0.07	4
			Spinel (1)[g]	0.01	20.40	+0.03	0.06	+0.01	0.05	4
			Duplicate			+0.04	0.08	+0.00	0.08	2
			Spinel (2)			+0.04	0.04	+0.03	0.05	2
			Average			+0.04	0.04	+0.02	0.03	
			Whole-rock[e]	1.00	44.50	−0.23	0.03	−0.15	0.07	
			Whole-rock[f]		44.50	−0.24	0.06	−0.11	0.05	4
HY2-14	Lherzolite	1055	Opx	0.23	33.29	−0.23	0.05	−0.11	0.05	4
			Cpx	0.10	15.76	−0.24	0.05	−0.11	0.03	10
			Olivine	0.66	50.09	−0.24	0.03	−0.14	0.01	4
			Spinel (1)	0.02	20.63	+0.11	0.06	+0.08	0.05	4
			Duplicate			+0.14	0.05	+0.11	0.04	2
			Spinel (2)			+0.16	0.10	+0.05	0.06	2
			Duplicate			+0.18	0.06	+0.04	0.06	2
			Average			+0.15	0.05	+0.07	0.02	
			Whole-rock[e]	1.00	42.40	−0.24	0.03	−0.14	0.01	
			Whole-rock[f]			−0.25	0.08	−0.12	0.05	4
HY2-03	Lherzolite	840	Opx	0.24	33.74	−0.25	0.05	−0.14	0.05	4
			Cpx	0.12	14.70	−0.15	0.02	−0.07	0.02	6
			Olivine	0.61	50.41	−0.26	0.08	−0.16	0.06	2
			Spinel (1)	0.03	20.79	+0.22	0.06	+0.13	0.05	4
			Spinel (2)			+0.25	0.04	+0.11	0.05	2
			Average			+0.23	0.03	+0.12	0.02	
			Whole-rock[e]	1.00	41.20	−0.25	0.05	−0.15	0.05	
			Whole-rock[f]			−0.23	0.09	−0.12	0.05	
HY2-05	Harzburgite	973	Opx	0.22	34.26	−0.24	0.02	−0.11	0.04	6
			Cpx	0.03	16.40	−0.19	0.03	−0.10	0.02	6
			Olivine	0.75	50.72	−0.22	0.05	−0.11	0.05	6
			Spinel (1)	0.01	19.41	+0.15	0.06	+0.08	0.05	4
			Spinel (2)			+0.10	0.06	+0.06	0.06	2
			Duplicate			+0.05	0.07	+0.02	0.06	2
			Average			+0.10	0.02	+0.05	0.02	
			Whole-rock[e]	1.00	45.80	−0.22	0.05	−0.11	0.05	
			Whole-rock[f]			−0.23	0.08	−0.12	0.05	4
HY2-07	Lherzolite	1150	Opx	0.30	32.07	−0.22	0.04	−0.11	0.04	4
			Cpx	0.16	16.07	−0.22	0.03	−0.10	0.02	6
			Olivine	0.52	49.64	−0.24	0.05	−0.15	0.04	4
			Spinel (1)	0.03	21.48	+0.06	0.04	+0.01	0.05	2
			Spinel (2)			+0.09	0.07	+0.04	0.05	4
			Duplicate			+0.06	0.10	+0.03	0.06	2
			Spinel (3)			+0.12	0.10	+0.04	0.06	2
			Duplicate			+0.15	0.06	+0.10	0.06	2
			Average			+0.09	0.05	+0.04	0.02	
			Whole-rock[e]	1.00	38.40	−0.23	0.05	−0.14	0.04	
			Whole-rock[f]			−0.21	0.08	−0.10	0.05	4
HY2-29	Lherzolite	1038	Opx	0.31	33.27	−0.25	0.07	−0.12	0.05	2
			Cpx	0.14	15.15	−0.24	0.03	−0.12	0.02	8
			Olivine	0.52	49.93	−0.29	0.05	−0.19	0.05	4
			Spinel (1)	0.03	22.34	+0.17	0.06	+0.09	0.05	6
			Duplicate			+0.17	0.08	+0.09	0.08	4
			Spinel (2)			+0.11	0.07	+0.07	0.05	2
			Duplicate			+0.13	0.10	+0.09	0.06	4
			Average			+0.14	0.03	0.09	0.03	
			Whole-rock[e]	1.00	38.60	−0.27	0.05	−0.16	0.05	
			Whole-rock[f]			−0.22	0.08	−0.09	0.05	4
HY2-06	Lherzolite	807	Opx	0.23	34.33	−0.26	0.07	−0.13	0.05	2
			Cpx	0.05	15.12	−0.14	0.05	−0.08	0.05	6
			Olivine	0.68	49.52	−0.27	0.05	−0.14	0.05	4
			Spinel (1)	0.03	20.25	+0.28	0.05	+0.17	0.04	2
			Spinel (2)			+0.25	0.06	+0.14	0.05	4
			Replicate[h]			+0.16	0.07	+0.05	0.05	4
			Average			+0.27	0.02	+0.09	0.04	
			Whole-rock[e]	1.00	38.40	−0.26	0.05	−0.14	0.05	

Table 2 (*continued*)

Sample	Rock type	T (°C)[a]	Mineral[b]	Modal	MgO	δ^{26}Mg	2 SD	δ^{25}Mg	2 SD	N[c]
Kuandian										
HY2-06			Whole-rock[f]			−0.27	0.08	−0.15	0.05	4
HY2-02	Lherzolite	1027	Opx	0.25	32.91	−0.28	0.03	−0.12	0.03	4
			Cpx	0.12	15.58	−0.22	0.05	−0.08	0.02	4
			Olivine	0.61	49.19	−0.28	0.05	−0.13	0.05	4
			Spinel (1)	0.02	21.01	+0.11	0.07	+0.05	0.05	4
			Replicate			+0.06	0.04	+0.02	0.05	2
			Spinel (2)			+0.12	0.06	+0.07	0.06	2
			Spinel (3)			+0.10	0.07	+0.04	0.05	4
			Average			+0.11	0.03	+0.05	0.02	
			Whole-rock[e]	1.00	40.20	−0.27	0.05	−0.13	0.05	
			Whole-rock[f]			−0.26	0.06	−0.14	0.05	4
HY2-04	Lherzolite	925	Opx	0.26	33.81	−0.24	0.07	−0.08	0.05	2
			Cpx	0.11	15.89	−0.18	0.05	−0.10	0.02	4
			Olivine	0.60	50.06	−0.28	0.05	−0.14	0.05	4
			Spinel	0.02	21.12	+0.14	0.04	+0.05	0.05	2
			Whole-rock[e]	1.00	40.7	−0.27	0.05	−0.13	0.05	
			Whole-rock[f]			−0.27	0.08	−0.15	0.05	4
Hannuoba										
DMP06-50	Clinopyroxenite	965	Opx	0.02	33.34	−0.23	0.06	−0.12	0.05	2
			Replicate			−0.26	0.09	−0.14	0.09	3
			Cpx	0.60	17.17	−0.19	0.11	−0.08	0.12	2
			Replicate			−0.19	0.11	−0.08	0.12	3
			Olivine[i]	0.20	50	−0.22	0.02	−0.15	0.02	2
			Replicate			−0.22	0.09	−0.17	0.02	3
			Phlogopite	0.13	20.61	−0.11	0.06	−0.05	0.05	5
			Whole-rock[e]			−0.19	0.06	−0.11	0.07	4
Sanyitang										
SYT06-41	Lherzolite	941	Opx (**Y**)[j]	0.15	33.61	−0.19	0.07	−0.07	0.03	4
			Cpx (**Y**)	0.13	16.34	−0.26	0.04	−0.12	0.05	4
			Replicate			−0.22	0.08	−0.13	0.08	2
			Olivine (**Y**)	0.60	49.40	−0.25	0.12	−0.14	0.08	4
			Replicate			−0.24	0.06	−0.11	0.06	2
			Phlogopite	0.10	20.85	−0.02	0.08	−0.01	0.08	4
			Replicate			−0.08	0.06	−0.03	0.03	2
			average			−0.05	0.05	−0.02	0.04	6
			Whole-rock[f]			−0.23	0.11	−0.12	0.07	
SYT06-42	Lherzolite	945	Opx (**Y**)	0.17	33.69	−0.23	0.07	−0.14	0.09	4
			Cpx (**Y**)	0.10	16.90	−0.20	0.07	−0.10	0.08	5
			Replicate			−0.18	0.06	−0.09	0.05	2
			Olivine (**Y**)	0.58	49.14	−0.28	0.13	−0.16	0.10	4
			Replicate			−0.28	0.06	−0.12	0.05	2
			Phlogopite	0.13	21.13	−0.14	0.06	−0.04	0.05	3
			Replicate			−0.19	0.06	−0.08	0.06	2
			average			−0.16	0.05	−0.06	0.04	5
			Whole-rock[f]			−0.26	0.11	−0.15	0.09	

[a] Temperatures were taken from Wu et al. (2006) and Zhao et al. (2007), which were calculated based on the two-pyroxene Ca thermometry (Brey and Köhler, 1990).
[b] Abbreviation: Cpx = clinopyroxene, Opx = orthopyroxene.
[c] N denotes the total run times of per newly purified sample solution by MC-ICPMS.
[d] Duplicate: repeated measurement of Mg isotopic ratios on the same purified solutions.
[e] Whole-rock Mg isotopic compositions that are calculated based on mineral data.
[f] Whole-rock Mg isotopic compositions that were previously reported in Teng et al. (2010a).
[g] The number in the bracket denotes different batches of spinel grains from the same peridotites. Each batch contains about 6–8 grains which weighted 1–2 mg.
[h] Replicate: repeat sample dissolution, column chemistry and instrumental analysis.
[i] MgO content of olivine in sample DMP06-50 is not available and is assumed to be 50 wt.%.
[j] Magnesium isotopic data of Ol, Opx, and Cpx separates from two Sanyitang peridotites (SYT06-41 and SYT06-42) reported in Yang et al. (2009), as marked as "**Y**". We re-measured Ol and Cpx from the two peridotites and measured phlogopite separates in this study.

5.2. Magnesium isotope fractionation between silicates in peridotite and clinopyroxenite xenoliths

5.2.1. Orthopyroxene versus olivine

Coexisting Opx and Ol from all analyzed peridotites have indistinguishable Mg isotopic compositions ($\Delta^{26}Mg_{Opx-Ol}$ = −0.04 to +0.04‰; n = 11) over the entire temperature range of ~350 °C (Fig. 2a), suggesting that there is no measurable Mg isotope fractionation between coexisting Opx and Ol, at temperature down to ~800 °C.

Previously reported Mg isotopic data for Opx–Ol pairs from peridotite xenoliths are summarized in Fig. 5a together with data reported here. Except one sample reported by Young et al. (2009), $\Delta^{26}Mg_{Opx-Ol}$ fractionations from other studies and this study are all smaller than +0.12‰ (Fig. 5a) and the mean is +0.03‰ (n = 31). Such small differences cannot be clearly resolved at current analytical uncertainties (±0.07‰ for δ^{26}Mg or ~±0.10‰ for Δ^{26}Mg; 2 SD). A quantitative estimate by Schauble (2011) predicts <+0.07‰ equilibrium Mg isotope fractionation between Opx and Ol at temperatures greater than 800 °C, e.g., +0.05‰ at 1000 °C, which agrees with these

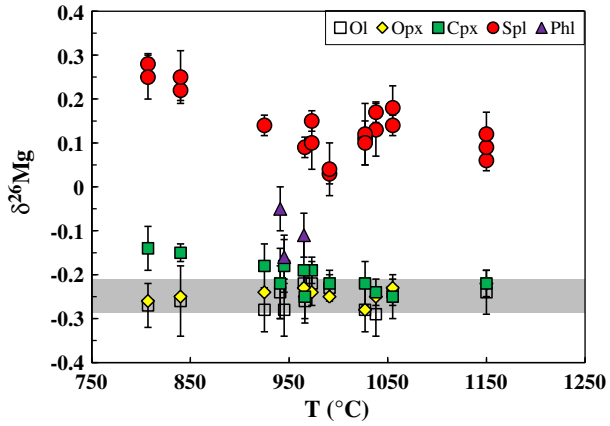

Fig. 1. Magnesium isotopic composition of mineral separates from peridotite and clinopyroxenite xenoliths from the North China craton as a function of estimated equilibrium temperatures. The gray bar represents the average Mg isotopic composition of global peridotites ($\delta^{26}Mg = -0.25 \pm 0.04$; Teng et al., 2010a). Magnesium isotopic data and equilibrium temperatures are reported in Table 2. Error bars in this figure represent 2 SD uncertainties.

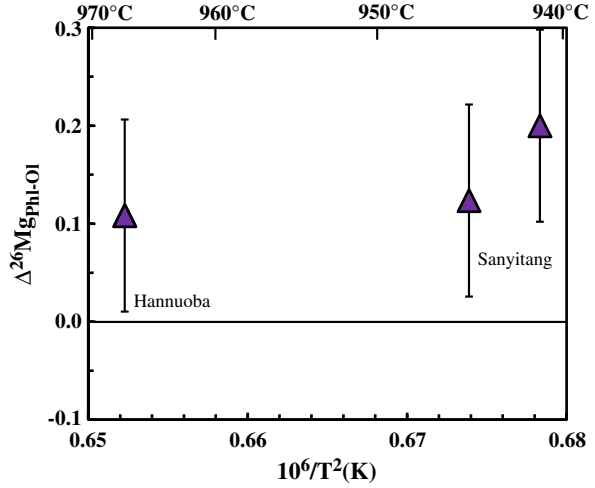

Fig. 3. Correlation of inter-mineral Mg isotope fractionation between phlogopite (Phl) and olivine (Ol) with $10^6/T^2$ (K) for Hannuoba olivine–clinopyroxenite and Sanyitang peridotite xenoliths. Data are reported in Table 2.

observations on natural samples. The sample with the largest $\Delta^{26}Mg_{Opx-Ol}$ value (+0.2‰) reported in Young et al. (2009) was interpreted as a result of disequilibrium isotope fractionation.

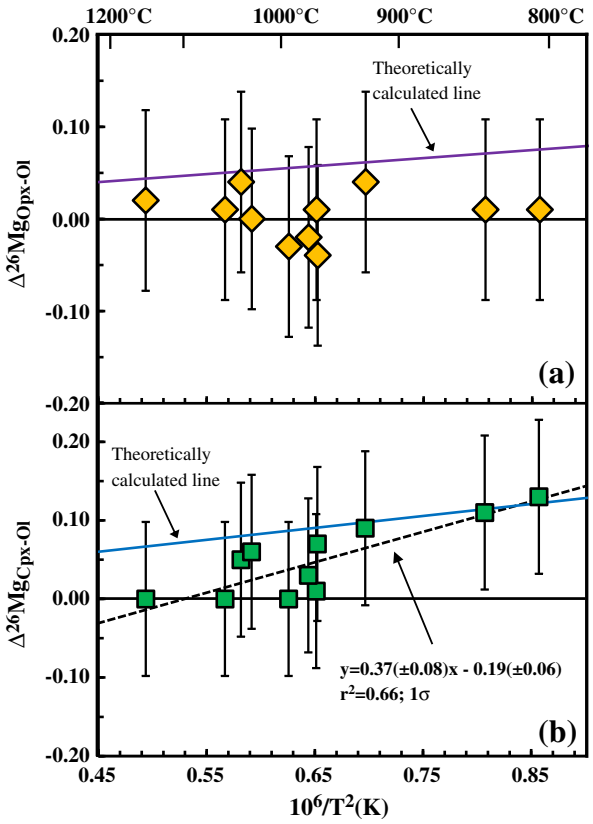

Fig. 2. Correlations of inter-mineral Mg isotope fractionation between pyroxene and olivine with $10^6/T^2$(K) for Kuandian peridotite and Hannuoba olivine–clinopyroxenite xenoliths, where T is the estimated equilibrium temperature. (a) Orthopyroxene (Opx) versus olivine (Ol); (b) clinopyroxene (Cpx) versus olivine (Ol). The theoretically calculated lines of Schauble (2011) are also plotted for comparison. Data are reported in Table 2. Uncertainties of $\Delta^{26}Mg$ values in this and all later figures quote 2 SD and are calculated based on the long-term external uncertainties of $\delta^{26}Mg$ measurement, i.e., $\pm 0.10‰ = \sqrt{2} \cdot (\pm 0.07‰)$.

5.2.2. Clinopyroxene versus olivine

Different from orthopyroxene, clinopyroxene appears to have slightly heavier Mg isotopic composition than coexisting olivine (Fig. 2b). The $\Delta^{26}Mg_{Cpx-Ol}$ values display a strong positive correlation with $10^6/T^2$(K) (Fig. 2b). Although some of these peridotites analyzed here were subjected to metasomatism by melt–rock interactions (Wu et al., 2006; Zhao et al., 2007), which could potentially affect Mg isotopic compositions of clinopyroxene and result in kinetic isotope fractionation, the lack of correlation between $\Delta^{26}Mg_{Cpx-Ol}$ and La/Sm ratio of clinopyroxenes or bulk peridotites (not shown), an indicator of mantle metasomatism, rules out mantle metasomatism as the principal cause of the Cpx–Ol Mg isotope fractionation. Instead, the correlation of inter-mineral isotope fractionation with temperature suggests equilibrium isotope fractionation. This is further supported by the agreement between measured $\Delta^{26}Mg_{Cpx-Ol}$ and theoretical predicted values (Fig. 2b). All $\Delta^{26}Mg_{Cpx-Ol}$ values fall on the theoretically predicated fractionation line within errors (Schauble,

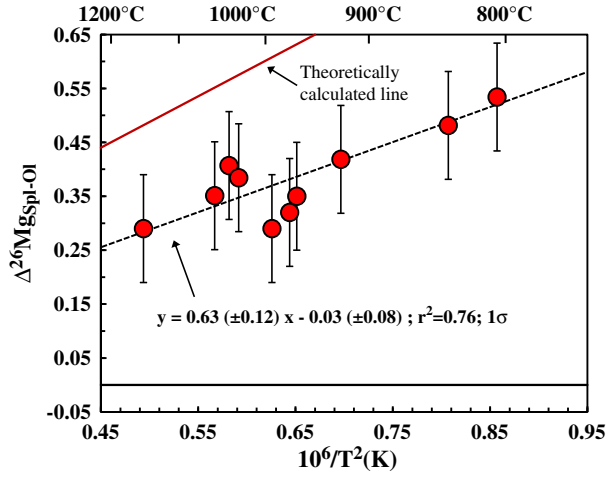

Fig. 4. Correlation of inter-mineral Mg isotope fractionation between spinel (Spl) and olivine (Ol) with $10^6/T^2$ (K) for Kuandian peridotite xenoliths. The temperature-dependent Spl–Ol Mg isotope fractionation factor is obtained using the least square fitting, where $10^3 \ln\alpha_{Spl-Ol} \approx \Delta^{26}Mg_{Spl-Ol} = 0.63(\pm 0.12) \times 10^6/T^2(K) - 0.03(\pm 0.08)$. The uncertainty of data fitting is at the 1σ level. The average $\delta^{26}Mg$ value for spinel that was measured multiple times is used here. The theoretically calculated line of Schauble (2011) is also plotted for comparison. Data are reported in Table 2.

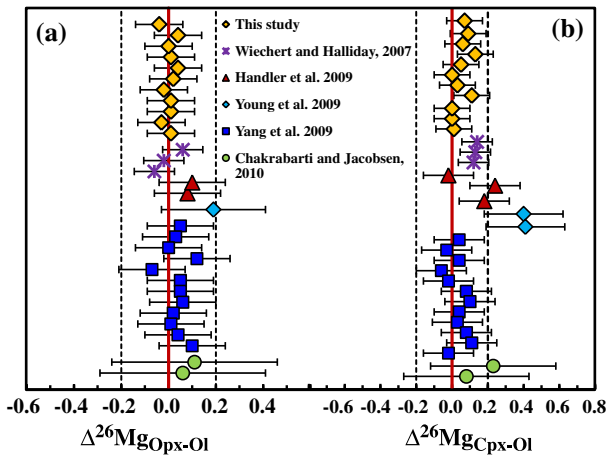

Fig. 5. A summary of Opx–Ol and Cpx–Ol Mg isotopic fractionation factors from published data and this study. For comparison, the 2 SD uncertainties for Δ^{26}Mg values are used here, which are calculated based on the external precision of δ^{26}Mg values for each study following the same formula in Fig. 2.

2011), suggesting an equilibrium Mg isotope fractionation between coexisting Cpx and Ol.

When compared to previous studies (Chakrabarti and Jacobsen, 2010; Handler et al., 2009; Wiechert and Halliday, 2007; Young et al., 2009), the direction of Mg isotope fractionation between Cpx and Ol is the same (i.e., Cpx is slightly heavier than coexisting Ol), whereas the magnitude of isotope fractionation varies significantly (>0.4‰ in $\Delta^{26}Mg_{Cpx-Ol}$ values) (Fig. 5b). These discrepancies are difficult to evaluate since the temperatures of most of those samples analyzed in previous studies were not reported. In addition, some isotope fractionations may reflect isotope disequilibrium due to mantle metasomatism (e.g., Young et al., 2009).

5.2.3. Phlogopite versus olivine

All three phlogopites from one clinopyroxenite and two lherzolites have Mg isotopic compositions heavier than coexisting olivines (Fig. 3). Because of the limited range of equilibrium temperatures among these three samples and the absence of theoretical or experimental calibrations for equilibrium Mg isotope fractionation factor between phlogopite and olivine, it is difficult to evaluate whether the Phl–Ol Mg isotope fractionation is in equilibrium or not. Nevertheless, the all positive $\Delta^{26}Mg_{Phl-Ol}$ values and their rough positive correlation with $10^6/T^2(K)$ (Fig. 3) appear to hint an equilibrium inter-mineral isotope fractionation. This is also in agreement with the speculation from theoretical considerations based on Mg – O bonding strengths, as discussed above. However, given that phlogopite in fertile peridotites is generally considered as products of mantle metasomatism (Menzies and Murthy, 1980; Prouteau et al., 2001), kinetic fractionations associated with melt–rock interactions cannot be fully excluded.

5.3. Spinel–olivine magnesium isotope fractionation in peridotite xenoliths

All spinels analyzed here have variable and significantly heavier Mg isotopic compositions than coexisting olivines (Fig. 4). Since δ^{26}Mg values of olivines are relatively constant (Fig. 1), the significant variation in $\Delta^{26}Mg_{Spl-Ol}$ value mainly reflects the variation in δ^{26}Mg of spinel. The large δ^{26}Mg variation in spinel relative to olivine reflects the negligible effect of spinel–olivine isotope exchange on Mg isotopic systematics of olivines because of the dilution effect. Compared to surrounding olivines, spinels are fewer and have lower Mg concentration, hence lower amount of Mg in the bulk peridotites.

5.3.1. Equilibrium magnesium isotope fractionation between spinel and olivine

Although no experimentally calibrated fractionation factor is available, several lines of evidence below suggest that the large Mg isotope fractionation between Spl and Ol in this study reflects equilibrium isotope fractionation.

Magnesium isotope fractionation between coexisting Spl and Ol is temperature dependent, with $10^3\ln\alpha_{Spl-Ol} \approx \Delta^{26}Mg_{Spl-Ol} = 0.63(\pm0.12)\times10^6/T^2(K) - 0.03(\pm0.08)$ (Fig. 4). The fitted line passes through the origin in the plot of $\Delta^{26}Mg_{Spl-Ol}$ vs. $10^6/T^2(K)$, as also indicated by the last term in the equation. This means that when temperature reaches infinitely high, the inter-mineral isotope fractionation factor ($\Delta^{26}Mg_{Spl-Ol}$) will be zero. The temperature-dependent isotope fractionation, therefore, strongly implies that coexisting spinels and olivines are in Mg isotope exchange equilibrium.

The equilibrium Spl–Ol Mg isotope fractionation is also consistent with the lack of correlation between $\Delta^{26}Mg_{Spl-Ol}$ values and chemical compositions of spinel and olivine (Fig. 6). In addition, in-situ analysis reveals that Spl, Ol, Opx and Cpx in Kuandian peridotites have relatively homogeneous Mg concentrations, without compositional zoning (Wu et al., 2006). Finally, identical Mg isotopic composition for different batches (6–8 grains) of spinels from the same xenolith sample (Fig. 1) indicates a lack of intra-mineral Mg isotopic variation and that Mg isotopes have reached exchange equilibrium within individual samples. All above evidences suggest an equilibrium Mg isotope fractionation between coexisting Spl and Ol in Kuandian peridotites.

Further support for Spl–Ol isotope equilibrium comes from quantitative diffusion calculations. The self-diffusion coefficient of Mg, D(Mg), in spinel (1.4×10^{-12} cm^2/s at 1200 °C) is about 2 orders of magnitude greater than that in olivine (~1.0×10^{-14} cm^2/s at 1200 °C) (Chakraborty et al., 1994; Liermann and Ganguly, 2002). By applying the characteristic diffusion length equation: $L = 2\sqrt{Dt}$, where L is the characteristic diffusion length and t is the diffusion time, the L will be

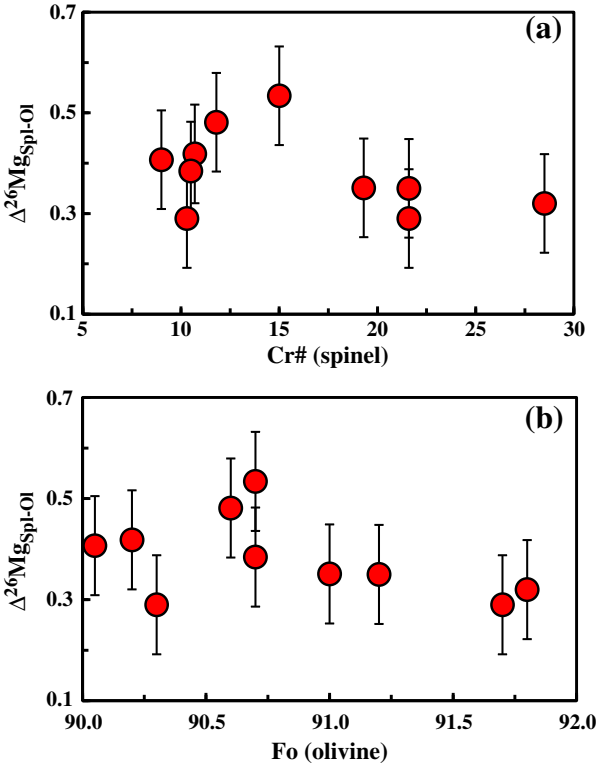

Fig. 6. Inter-mineral Mg isotope fractionation between spinel and olivine with (a) Cr# of spinel and (b) Fo composition of olivines from the Kuandian peridotites. Magnesium isotopic data are reported in Table 2. Spinel Cr# and olivine Fo are from Wu et al. (2006).

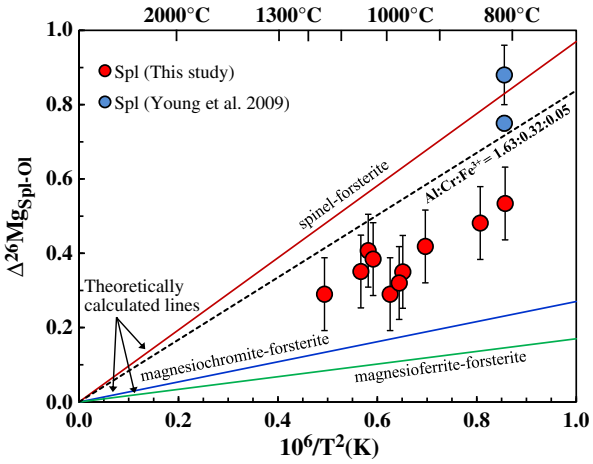

Fig. 7. Comparison of measured Spl–Ol Mg isotope fractionation with theoretical predictions as a function of temperature. Theoretical calculations for pure spinel, magnesiochromite and magnesioferrite end members are from Schauble (2011). The dotted line represents the fractionation line calculated for our samples based on their Al:Cr:Fe^{3+} ratios (Table 3). The offset between our results and the calculated fractionation line reflects an additional effect of Mg coordination numbers in spinels on Mg isotopic composition of spinels. See text for the details.

1 cm in olivine after 3 m.y. diffusion at 1200 °C. The diffusion length in spinel at the same diffusion time is about 10 times longer i.e., >10 cm. Hence, the maximum time required for Mg diffusion equilibrium between existing spinel and olivine is a few million years or less, at mantle temperature. Studies of Re–Os isotopic systematics in Kuandian peridotite xenoliths indicate that melt extraction occurred as early as ~1.9 Ga (Wu et al., 2006). Therefore, these xenoliths were in the mantle for more than one thousand million years before they were brought to surface through the Cenozoic eruption, and Mg diffusion equilibrium should have reached between spinel and olivine over such a long time scale.

5.3.2. Comparison with Spl–Ol fractionation in San Carlos peridotite xenoliths

When compared to our data, the $\Delta^{26}Mg_{Spl-Ol}$ values (+0.75 and +0.88‰) in two San Carlos peridotites reported in Young et al. (2009) are larger and fall above the positive trend defined by our samples (Fig. 7). Below we explore the possible reasons for this discrepancy.

One reason may be due to the use of different thermometers. Thermometer used here is the two-pyroxene Ca thermometer (Brey and Köhler, 1990), whereas that used for comparison in Young et al. (2009) is the closure temperature (T_c) obtained from inversion parameters in spinels, which is 808 ± 37 °C for "Group I" xenolith (note: not the same sample as analyzed in Young et al., 2009). In this case, if spinel and olivine samples from both Young et al. (2009) and this study are in isotope equilibrium, then the two-pyroxene temperature needs to be ~200 °C lower than the closure temperature obtained from inversion parameters in spinels. However, such difference is unlikely since the two-pyroxene equilibrium temperature for the San Carlos spinel lherzolite (~1050 °C) estimated by Brey and Köhler (1990) is even higher than the closure temperature.

Another possibility is that isotope fractionation reported in one of these two studies is not in equilibrium. One important criteria to evaluate whether isotope equilibrium is reached or not is to check whether the isotope fractionation is temperature-dependent or not. Given the large temperature range of our samples (~350 °C), isotope equilibrium in these samples is well demonstrated by the positive correlation between $\Delta^{26}Mg_{Spl-Ol}$ and $10^6/T^2(K)$ (Fig. 4) as well as the lack of intra-mineral isotopic variation (Fig. 1). By contrast, Young et al. (2009) measured spinels from two samples that formed at similar temperatures, thus it is difficult to evaluate the effect of temperature. Furthermore, the $\delta^{26}Mg$ offsets between Opx/Cpx and Ol from the two San Carlos peridotites in Young et al. (2009) are also 0.2–0.3‰ higher than our results, which Young et al. (2009) interpreted as a result of isotopic disequilibrium.

5.3.3. Comparison with theoretical study

Compared to theoretical studies of inter-mineral Mg isotope fractionation by Schauble (2011), our results are broadly similar for Opx–Ol and Cpx–Ol pairs (Fig. 2a, b) but systemically lower for Spl–Ol pairs (Fig. 7). Fitting our Spl–Ol data on the theoretically calculated line would yield isotope exchange temperatures ranging from ~1000 to 1600 °C, which are over 200 °C higher than the two-pyroxene equilibrium temperatures. Such temperatures are too high to be realistic. We infer that the discrepancy reflects the complicated effects of chemical composition of spinels on theoretically calculated Mg isotope fractionation factors between Spl and Ol.

Schauble (2011) pointed out that there were at least five factors which can substantially impact the estimates. In particular, partitioning of Mg isotopes in natural spinel ($A^{2+}B_2^{3+}O_4^{2-}$) strongly depends on the octahedral ion composition (i.e., B^{3+}). For example, the reduced partition function ratios for $^{26}Mg/^{24}Mg$, $1000\cdot\ln(\beta_{26-24})$, vary significantly from pure spinel ($MgAl_2O_4$, 3.38), through magnesiochromite ($MgCr_2O_4$, 2.68), to magnesioferrite ($MgFe_2O_4$, 2.58) at 1000 K, due to the different octahedral cation compositions (Schauble, 2011). As a result, the equilibrium $\Delta^{26}Mg$ fractionation between pure spinel and forsterite is ~+1.0‰ whereas the fractionations between magnesiochromite and forsterite and between magnesioferrite and forsterite are only ~+0.30‰ and ~+0.20‰, respectively (Fig. 7). Consequently, natural spinels that contain these three components

Table 3
Chemical formula of spinels from the Kuandian peridotites.

Sample	HY1-01	HY2-01	HY2-02	HY2-03	HY2-04	HY2-05	HY2-06	HY2-07	HY2-14	HY2-29	Mean
Ti^{4+}	0.002	0.001	0.001	0.001	0.000	0.002	0.001	0.003	0.002	0.002	0.002
Al^{3+}	1.437	1.524	1.742	1.733	1.749	1.392	1.664	1.733	1.566	1.765	1.631
Cr^{3+}	0.494	0.421	0.204	0.232	0.210	0.555	0.293	0.198	0.374	0.175	0.316
Fe^{3+}	0.064	0.054	0.052	0.034	0.041	0.049	0.041	0.063	0.055	0.056	0.051
Fe^{2+}	0.177	0.197	0.181	0.189	0.185	0.218	0.209	0.185	0.189	0.169	0.190
Ni^{2+}	0.004	0.006	0.008	0.005	0.007	0.006	0.006	0.005	0.007	0.007	0.006
Mn^{2+}	0.004	0.004	0.003	0.003	0.004	0.006	0.004	0.004	0.003	0.001	0.004
Mg^{2+}	0.808	0.793	0.804	0.802	0.802	0.766	0.781	0.807	0.799	0.823	0.799
Ca^{2+}	0.002	0.000	0.001	0.000	0.000	0.000	0.000	0.000	0.000	0.000	0.000
Na^{+}	0.004	0.000	0.001	0.001	0.001	0.002	0.000	0.000	0.000	0.000	0.001
K^{+}	0.001	0.000	0.002	0.000	0.001	0.001	0.000	0.000	0.001	0.000	0.001
Tot. Cat.	3.000	3.000	3.000	3.000	3.000	3.000	3.000	3.000	3.000	3.000	3.000
Tot. Oxy.	4.000	4.000	4.000	4.000	4.000	4.000	4.000	4.000	4.000	4.000	4.000

The cations in per formula unit were calculated from chemical compositions of spinels reported in Wu et al. (2006). Original iron contents were measured as total FeO and here the Fe^{2+} and Fe^{3+} species are calculated based on charge balance law.

should have $\Delta^{26}Mg_{Spl-Ol}$ values falling between +1.0‰ and +0.2‰ at 1000 K. Extrapolation of the linear relationship for our samples in Fig. 4 suggests a $\Delta^{26}Mg_{Spl-Ol}$ fractionation of +0.6‰ at 1000 K, which is within this expected range (Fig. 7).

In detail, spinels from Kuandian peridotites have a general formula of $(Mg_{0.80}Fe^{2+}_{0.19}Ni_{0.01})^{IV}(Al_{1.63}Cr_{0.32}Fe^{3+}_{0.05})^{VI}O_4$ (Table 3), which clearly shows the presence of a significant amount of magnesiochromite and minor magnesioferrite species. This is also the case for San Carlos spinels that have a typical formula of $(Mg_{0.73}Fe^{2+}_{0.27})^{IV}(Al_{1.19}Cr_{0.74}Fe^{3+}_{0.06})^{VI}O_4$ (Young et al., 2009). Therefore, contributions from these three end members of pure spinel, magnesiochromite and magnesioferrite need be taken into account when comparing theoretical calculation with natural data. Based on the relative proportions of the three different end members in our samples, we calculate the average $\Delta^{26}Mg_{Spl-Ol}$ value at 1000 K is ~+0.8‰. The calculated value is closer to, but still slightly greater than our measurements (Fig. 7). The small difference might reflect an additional effect from substitution of ions in octahedral sites with those in tetrahedral sites in natural spinels.

Different from silicates, substitution of B^{3+} ions in octahedral sites with A^{2+} ions in tetrahedral sites is common for natural spinels, and Mg^{2+} in spinel occupies both tetrahedral and octahedral sites where the relative proportion is determined by inversion parameter *i* (e.g., Sickafus et al., 1999). Partitioning of Mg isotopes in spinel also strongly depends on the octahedral substitution (Schauble, 2011). Theoretical calculations in Schauble (2011) were based on the assumption that all Mg is in tetrahedral sites in pure spinel, magnesiochromite and magnesioferrite species. Thus, the results calculated from normal (tetrahedral) spinel/magnesiochromite/magnesioferrite would overestimate the $\Delta^{26}Mg_{Spl-Ol}$ fractionation factors for natural spinels, because octahedral sites potentially favor isotopically lighter Mg isotopes than tetrahedral sites. It is more difficult to quantify the effects of the inversion parameter on the overall $\Delta^{26}Mg_{Spl-Ol}$ fractionation for natural spinels but this could qualitatively explain why there is still a difference between measurements on natural samples and theoretical calculations of Spl–Ol fractionation after correction of the effects of spinel compositions.

5.3.4. Spl–Ol magnesium isotope geothermometry

Spinel constitutes one of the most important phases in the shallow upper mantle, and the Fe^{2+}–Mg inter-diffusion in spinel from mantle rocks has been widely applied as geothermometry (Fabriès, 1979; Lehmann, 1983; Liermann and Ganguly, 2002) and geospeedometry (e.g., Ozawa, 1984). Compared to the Fe^{2+}–Mg inter-diffusion in spinel, however, the spinel–olivine Mg isotope geothermometry may have a greater potential, because the former is more sensitive to concentration estimate of Fe^{2+} and Fe^{3+} species in spinel (See Young et al., 2009 for more details). The large equilibrium Spl–Ol Mg isotope fractionation in mantle rocks demonstrated here, $10^3\ln\alpha_{Spl-Ol} \approx \Delta^{26}Mg_{Spl-Ol} = 0.63(\pm0.12)\times10^6/T^2(K) - 0.03(\pm0.08)$ (Fig. 4), thus, highlights its potential application as a new geothermometry in mantle geochemistry.

As highlighted in the previous discussion, chemical compositions of spinels play an important role on Mg isotope fractionation between Spl and Ol. Hence, when applying Spl–Ol Mg isotope geothermometry, caution should be taken while calculating temperatures from measured $\Delta^{26}Mg_{Spl-Ol}$ values by directly following theoretical calculations and without considering the detailed chemical compositions of spinels in natural samples.

5.4. Implications for Mg isotopic composition of the Earth and terrestrial planets

Compared to measured δ^{26}Mg values of bulk peridotites (Teng et al., 2010a), the calculated whole-rock values, based on Mg concentrations, isotopic compositions and modes of mineral separates, are identical (Table 2). δ^{26}Mg of measured olivine separates are similar to values of bulk peridotites, suggesting that olivines dominate the Mg budget of bulk peridotites. However, in the olivine clinopyroxenite from Hannuoba, the calculated whole-rock δ^{26}Mg value of −0.19‰ is slightly heavier than that of olivine (Table 2), reflecting its high modes of clinopyroxene (60%) and phlogopite (13%), both of which have heavier Mg isotopic compositions ($\delta^{26}Mg = -0.19$‰ and −0.11‰ respectively) than coexisting olivine ($\delta^{26}Mg = -0.22$‰).

Our results suggest that δ^{26}Mg of olivine can represent that of bulk peridotites when the mode of olivine (e.g., dunite, lherzolite, and harzburgite) is high, but might not represent that of highly fertile peridotites with a large volume of clinopyroxene and phlogopite, due to the small inter-mineral Mg isotope fractionations between Cpx/Phl and Ol. In addition, isotopically distinct melts may be produced by differential melting of peridotites since melts produced by melting of phlogopite and clinopyroxene should be isotopically heavier than those by olivines. Hence, future studies on comparison of Mg isotopic composition between differentiated planetary bodies in the solar nebula need to take into account the small but measurable inter-mineral Mg isotope fractionation.

Nonetheless, regardless of various chemical compositions and lithologies, peridotite and clinopyroxenite xenoliths from the North China craton have Mg isotopic compositions, on average, similar to those of chondrites (Schiller et al., 2010; Teng et al., 2010a), suggesting a chondritic Mg isotopic composition of the silicate Earth.

6. Conclusions

High-precision Mg isotopic data are reported for coexisting mantle minerals (Ol, Opx, Cpx, Phl and Spl) from a suite of mantle xenoliths from the North China craton that formed over a large temperature range from 807 to 1150 °C. The major conclusions are:

(1) Opx has Mg isotopic composition similar to coexisting olivine over the entire temperature range, with $\Delta^{26}Mg_{Opx-Ol} = -0.4$ to +0.4‰ (n = 11).
(2) Cpx appears to be slightly heavier ($\Delta^{26}Mg_{Cpx-Ol} = 0$ to +0.13‰, n = 13) than coexisting olivine, with $\Delta^{26}Mg_{Cpx-Ol}$ positively correlated with $10^6/T^2$ (K), indicating equilibrium isotope fractionation.
(3) All phlogopites have Mg isotopic compositions heavier than coexisting olivines, with $\Delta^{26}Mg_{Phl-Ol} = +0.11$ to +0.20‰ (n = 3). The fractionation might reflect equilibrium isotope fractionation based on theoretical considerations but kinetic isotope fractionation associated with mantle metasomatism cannot be ruled out.
(4) Spinels have heavier Mg isotopic compositions relative to coexisting silicates, with $\Delta^{26}Mg_{Spl-Ol} = +0.25$ to +0.55‰ (n = 10). The positive correlation between $\Delta^{26}Mg_{Spl-Ol}$ and $10^6/T^2$ (K) [$\Delta^{26}Mg_{Spl-Ol} = 0.63(\pm0.12)\times10^6/T^2(K) - 0.03$ (±0.08)], the lack of intra-mineral fractionation and the relatively short time required for Mg diffusive equilibrium at mantle temperature, suggest that spinel and olivine are in Mg isotope equilibrium. The large equilibrium spinel–olivine Mg isotope fractionation may potentially be used as a new geothermometry in mantle geochemistry.
(5) Inter-mineral Mg isotope fractionation is primarily controlled by the Mg–O bonding strength. The observed magnitude of inter-mineral fractionation between mantle minerals agrees with theoretical estimates by Schauble (2011).
(6) Peridotite and clinopyroxenite xenoliths analyzed here have an average Mg isotopic composition similar to chondrites, suggesting a chondritic Mg isotopic composition of the Earth.

Acknowledgments

We thank Xinmiao Zhao for providing the Hannuoba samples, Shan Ke, Fatemeh Sedaghatpour, Wang-Ye Li for help in the lab, and Bill McDonough, Roberta Rudnick, Shuguang Li, Yan Xiao, Jingao Liu for stimulating discussions. Constructive comments from Philip Pogge von Strandmann, Edwin Schauble and an anonymous reviewer as well as careful handling by Rick Carlson are greatly appreciated. This work was financially supported by the National Science Foundation (EAR-0838227 and EAR-1056713) and Arkansas Space Grant Consortium (SW19002) S. A. L. is partially supported by the National Natural Science Foundation of China (40973016) and the China Scholarship Council.

References

Bigeleisen, J., Mayer, M.G., 1947. Calculation of equilibrium constants for isotopic exchange reactions. J. Chem. Phys. 15, 261–267.

Brey, G.P., Köhler, T., 1990. Geothermobarometry in four-phase lherzolites II. New thermobarometers, and practical assessment of existing thermobarometers. J. Petrol. 31, 1353–1378.

Chakrabarti, R., Jacobsen, S.B., 2010. The isotopic composition of magnesium in the inner Solar System. Earth Planet. Sci. Lett. 293, 349–358.

Chakraborty, S., Farver, J.R., Yund, R.A., Rubie, D.C., 1994. Mg tracer diffusion in synthetic forsterite and San Carlos olivine as a function of P, T and fO_2. Phys. Chem. Miner. 21, 489–500.

Fabriès, J., 1979. Spinel–olivine geothermometry in peridotites from ultramafic complexes. Contrib. Mineral. Petrol. 69, 329–336.

Foster, G.L., von Strandmann, P., Rae, J.W.B., 2010. Boron and magnesium isotopic composition of seawater. Geochem. Geophys. Geosyst. 11, 1–10.

Handler, M.R., Baker, J.A., Schiller, M., Bennett, V.C., Yaxley, G.M., 2009. Magnesium stable isotope composition of Earth's upper mantle. Earth Planet. Sci. Lett. 282, 306–313.

Huang, S., Farkas, J., Jacobsen, S.B., 2010. Calcium isotopic fractionation between clinopyroxene and orthopyroxene from mantle peridotites. Earth Planet. Sci. Lett. 292, 337–344.

Lehmann, J., 1983. Diffusion between olivine and spinel: application to geothermometry. Earth Planet. Sci. Lett. 64, 123–138.

Li, W.-Y., Teng, F.-Z., Ke, S., Rudnick, R.L., Gao, S., Wu, F.Y., Chappell, B.W., 2010. Heterogeneous magnesium isotopic composition of the upper continental crust. Geochim. Cosmochim. Acta 74, 6867–6884.

Li, W.-Y., Teng, F.-Z., Xiao, Y., Huang, J., 2011. High-temperature inter-mineral magnesium isotope fractionation in eclogite from the Dabie orogen, China. Earth Planet. Sci. Lett. 304, 224–230.

Liermann, H., Ganguly, J., 2002. Diffusion kinetics of Fe^{2+} and Mg in aluminous spinel: experimental determination and applications. Geochim. Cosmochim. Acta 66, 2903–2913.

Liu, S.-A., Teng, F.-Z., He, Y.-S., Ke, S., Li, S.-G., 2010. Investigation of magnesium isotope fractionation during granite differentiation: implication for Mg isotopic composition of the continental crust. Earth Planet. Sci. Lett. 297, 646–654.

Menzies, M.A., Murthy, V.R., 1980. Nd and Sr isotope geochemistry of hydrous mantle nodules and their host alkali basalts: implications for local heterogeneities in metasomatically veined mantle. Earth Planet. Sci. Lett. 46, 323–334.

Ozawa, K., 1984. Olivine–spinel geospeedometry: analysis of diffusion-controlled Mg–Fe^{2+} exchange. Geochim. Cosmochim. Acta. 48, 2597–2611.

Prouteau, G., Scaillet, B., Pichavant, M., Maury, R., 2001. Evidence for mantle metasomatism by hydrous silicic melts derived from subducted oceanic crust. Nature 40, 197–200.

Schauble, E., 2011. First-principles estimates of equilibrium magnesium isotope fractionation in silicate, oxide, carbonate and hexaaquamagnesium(2+) crystals. Geochim. Cosmochim. Acta 75, 844–869.

Schiller, M., Handler, M.R., Baker, J.A., 2010. High-precision Mg isotopic systematics of bulk chondrites. Earth Planet. Sci. Lett. 297, 165–173.

Shahar, A., Young, E.D., Manning, C.E., 2008. Equilibrium high-temperature Fe isotope fractionation between fayalite and magnetite: an experimental calibration. Earth Planet. Sci. Lett. 268, 330–338.

Sickafus, K.E., Wills, J.M., Grimes, J.W., 1999. Structure of spinel. J. Am. Ceram. Soc. 82, 3279–3292.

Teng, F.-Z., McDonough, W.F., Rudnick, R.L., Walker, R.J., Sirbescu, M.-L.C., 2006. Lithium isotopic systematics of granites and pegmatites from the Black Hill, South Dakota. Am. Mineral. 91, 1488–1498.

Teng, F.-Z., Wadhwa, M., Helz, R.T., 2007. Investigation of magnesium isotope fractionation during basalt differentiation: implications for a chondritic composition of the terrestrial mantle. Earth Planet. Sci. Lett. 261, 84–92.

Teng, F.-Z., Li, W.-Y., Ke, S., Marty, B., Dauphas, N., Huang, S., Wu, F.-Y., Pourmand, A., 2010a. Magnesium isotopic composition of the Earth and chondrites. Geochim. Cosmochim. Acta 74, 4150–4166.

Teng, F.-Z., Li, W.-Y., Rudnick, R.L., Gardner, L.R., 2010b. Contrasting lithium and magnesium isotope fractionation during continental weathering. Earth Planet. Sci. Lett. 300, 63–71.

Urey, H.C., 1947. The thermodynamic properties of isotopic substances. J. Chem. Soc. (London) 562–581.

Wiechert, U., Halliday, A.N., 2007. Non-chondritic magnesium and the origins of the inner terrestrial planets. Earth Planet. Sci. Lett. 256, 360–371.

Wu, F.-Y., Walker, R.J., Yang, Y.-H., Yuan, H.-L., Yang, J.-H., 2006. The chemical–temporal evolution of lithospheric mantle underlying the North China Craton. Geochim. Cosmochim. Acta 70, 5013–5034.

Yang, W., Teng, F.-Z., Zhang, H.-F., 2009. Chondritic magnesium isotopic composition of the terrestrial mantle: a case study of peridotite xenoliths from the North China craton. Earth Planet. Sci. Lett. 288, 475–482.

Young, E.D., Tonui, E., Manning, C.E., Schauble, E.A., Macris, C., 2009. Spinel–olivine magnesium isotope thermometry in the mantle and implications for the Mg isotopic composition of Earth. Earth Planet. Sci. Lett. 288, 524–533.

Zhao, X.M., Zhang, H.F., Zhu, X.K., Zhang, W.H., Yang, Y.H., Tang, Y.J., 2007. Metasomatism of Mesozoic and Cenozoic lithospheric mantle beneath the North China craton: evidence from phlogopite-bearing mantle xenoliths. Acta Petrol. Sin. 23, 1281–1293.